Determining Unbraced Lengths in Continuous Girders Subjected to Warping Restraint

C.E. Quadrato[1], K.P. Arnett[2]

Abstract
Both AASHTO and AISC provisions for flexural members assume that no warping restraint is provided to a member undergoing elastic lateral torsional buckling. And while AASHTO provisions allow for a rational analysis to determine required unbraced lengths, most transportation jurisdictions simply use previously mandated cross frame spacing requirements. However, ignoring warping restraint typically results in a very conservative critical span bracing pattern. Previous research has shown that elastic buckling strengths for critical spans increase from 30% to 50% due to the warping restraint provided by adjacent spans and can increase as much as 50% to 90% when a split pipe warp restraining device is used at the piers and abutments.

This study expands on previous laboratory and computational research conducted at the University of Texas at Austin Ferguson Structural Engineering Laboratory and The United States Military Academy by examining continuous girders subjected to distributed load patterns common in bridge and building construction. To conduct the study, previously validated finite element modeling techniques are used to estimate continuous girder buckling capacity and compare the results to a recently developed analytic procedure to account for warping and weak axis torsional restraint provided to the critical span by adjacent span and split pipe warping restraint devices.

1. Introduction
Previous computational studies conducted at the United States Military Academy have shown that accounting for the increase in continuous girder elastic buckling capacity due to warping restraint at the ends and piers required more than just considering the restraint provided by adjacent spans warping and weak axis rotation stiffness (Quadrato & Arnett, 2013). The moment gradient also played a key role in estimating this increase. This study examines the relationship between all three factors and proposes a method to estimate the maximum unbraced length for the critical span of a continuous steel girder. This study also considers the impact of split pipe warp restraining devices on the elastic critical girder buckling load in the critical span.

---

[1] Assistant Professor, United States Military Academy, <craig.quadrato@usma.edu>
[2] Instructor, United States Military Academy, <kevin.arnett@usma.edu>

2. Background

Girder elastic buckling strength and its associated critical unbraced length depend on the girder cross sectional geometry, support conditions, and load placement. Initial studies such as those done by Nethercot and Rockey (Nethercot & Rockey, 1971) provided accurate estimates using a single factor known as a buckling coefficient shown in Eq. 1

$$M_{cr} = \pi^2 \alpha / L_b \sqrt{EI_y GJ + \pi^2 E^2 C_W I_Y / L_b^2} \qquad (1)$$

where

M_{cr} = girder segment buckling moment
α = buckling coefficient
L_b = girder segment unbraced length
I_y = girder segment weak-axis moment of inertia
G = shear modulus
J = girder segment torsional constant
E = Young's modulus
C_w = girder segment warping constant

Another approach is to separate the modifiers for support conditions and load placement into two or more factors. The load placement effect factors are typically captured using a coefficient of bending and the support conditions are accounted for through one or two effective length factors as summarized in Guide to Stability Criteria for Metal Structures (Structural Stability Research Council, 1998) and shown in Eq. 2 (American Institute of Steel Construction, 2011) and (Trahair, 1993).

$$M_{cr} = \pi^2 C_b / (k_y L_b) \sqrt{EI_y GJ + \pi^2 E^2 C_W I_Y / (k_w L_b)^2} \qquad (2)$$

where

C_b = moment gradient coefficient
k_y = girder segment effective length factor for weak axis rotational restraint
k_w = girder segment effective length factor for warping restraint

In this approach, the moment gradient coefficient is calculated as shown below and accounts for nonuniform moment as well as load height effects (Structural Stability Research Council, 1998).

$$C_b = \frac{12.5 M_{max}}{2.5 M_{max} + 3 M_A + 4 M_B + 3 M_C} 1.4^{2y/h} \qquad (3)$$

where

M_{max} = maximum moment in the span
M_A, M_B, M_c = the moments at the ¼, ½, and ¾ points in the span, respectively
y = distance from load point to cross section mid-height (positive for below and negative for above cross section mid-height)
h = girder depth

The buckling coefficient approach has been shown to be extremely effective for specific boundary and loading conditions for which the coefficient, α, is derived. Expressions for α exist for simply supported, warping fixed, weak axis bending fixed, and rigid end conditions with mid-span concentrated, evenly spaced double concentrated loads, uniformly distributed, and end moment loading conditions at all heights along the cross section (Nethercot & Rockey, 1971). An example finite element model with its ends fixed against weak axis rotation and warping with a mid-span concentrated load shown below was run and compared to Eq. 1. The finite element model estimated the buckling load at 25.61 kips while Eq. 1 predicted 25.87 kips for a 1% difference. But, Eq. 2 gives the buckling estimate as 33.15 kips, an overestimate of over 28% when using $k_y = 0.5$ and $k_w = 0.5$. Similar errors were noted in other loading conditions and girder geometries investigated.
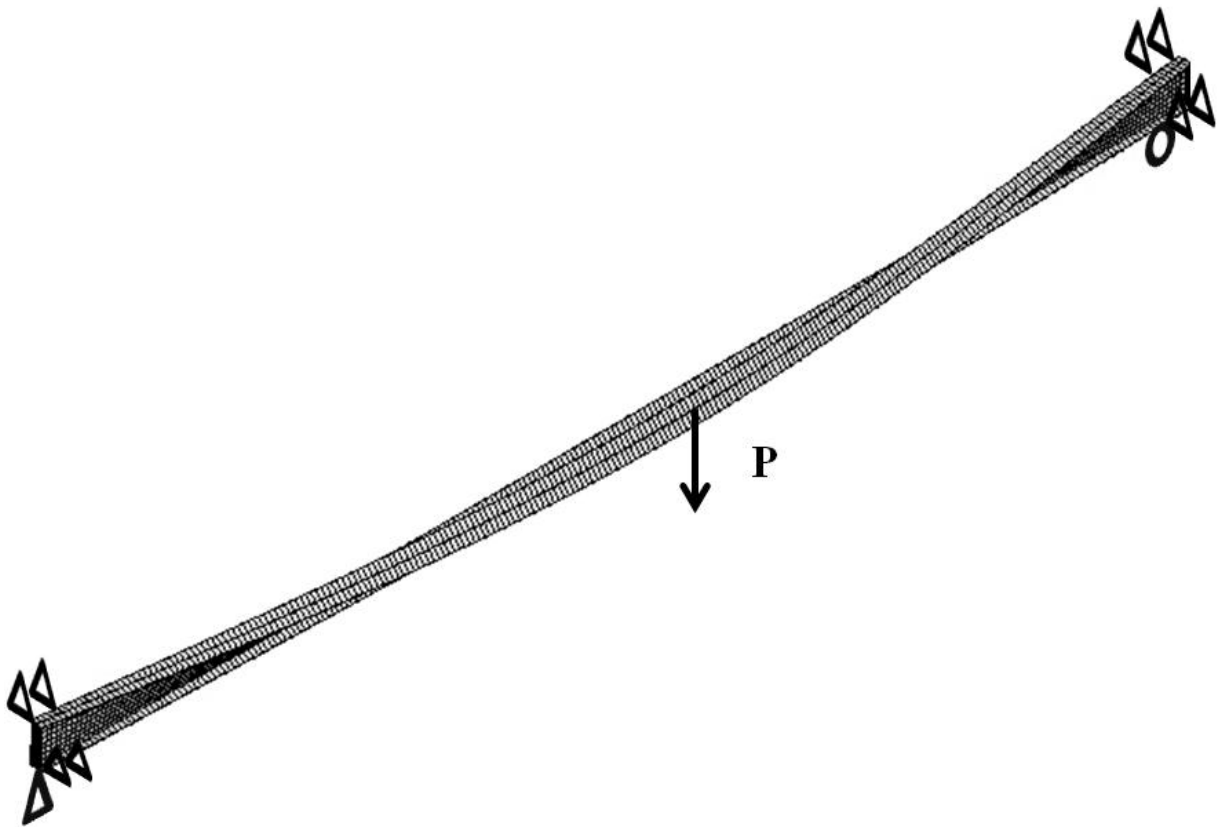
Figure 1: Single-Span Girder Buckled Shape

These results are not surprising as Eq. 1 was derived for these support conditions, while Eq. 2 assumes that the bending moment coefficient is independent of any applied warping or weak axis rotational restraint. However, deviating from the completely fixed conditions in the model induces significant errors in Eq. 1 and attempting to use Eq. 2 for situations with significant weak axis rotational and warping restraint leads to significant errors in estimating buckling strength (Quadrato & Arnett, 2013). The problem is further compounded when warp restraining devices, such as the split pipe stiffeners shown below are used to prevent warping.
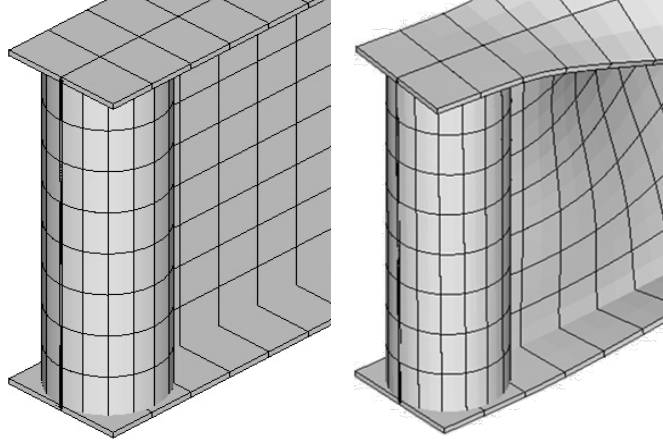
Figure 2: Split Pipe Stiffener Before (L) and After (R) Girder Buckling

3. Proposed Analytic Solution

The proposed initial analytic solution is to use the effective length factor approach of Eq. 2 combined with the buckling coefficient approach of Eq. 1. This allows the fully rigid conditions required in the buckling coefficient of Eq. 1 to be adjusted via the effective length factors used in Eq. 2. The proposed method is outlined below and relies on a similar method to determine the effective length factors for adjacent spans and warp restraining devices used in previous studies (Quadrato & Arnett, 2013) (Pi & Trahair, 2000) (Trahair, 1993).

1. Compute the girder strong axis bending moment diagram and find the maximum moment in each segment (M_{mi}) for the load condition to be investigated.

2. Calculate the effect of moment gradient and load height using Eq. 5 below for each segment assuming the segment is simply supported and initially assume effective length factors k_w and k_y are equal to one.

$$C_b = AB^x \tag{4}$$

where

$$A = \frac{12.5 M_{max}}{2.5 M_{max} + 3 M_A + 4 M_B + 3 M_C}$$

When calculating A use the simply supported moment diagram for spans loaded by applied loads.

B = 1-0.018W^2+0.649W for concentrated load at mid-span

B = 1-0.154W^2+0.535W for a uniformly distributed load along the span

(other B values are available from (Nethercot & Rockey, 1971) but this current study will be limited to the two loading conditions described above).

$$W = \pi/(k_y L_b)\sqrt{E C_w/(GJ)}$$

x = 1 for bottom flange loading; 0 for loads applied at the centroid, -1 for top flange loading

3. Determine the critical elastic buckling moment capacity (M_{cri}) for each unbraced segment using Eq. 2 (repeated below for convenience).

$$M_{cr} = \pi^2 C_b / (k_y L_b) \sqrt{EI_y GJ + \pi^2 E^2 C_W I_Y / (k_w L_b)^2} \qquad (4)$$

4. Determine each segment's remaining load capacity prior to elastic buckling for the loading condition to be investigated using Eq. 5 below. The highest value of λ will be the critical span (λ_c) and the segments adjacent to it will be the restraining segments $(\lambda_r)_{A/B}$ where A and B denote the segments on either side of the critical segment.

$$\lambda_i = M_{cri} / M_{mi} \qquad (5)$$

where

λ_i = segment buckling capacity factor – note that $\lambda_c = 1$ for the critical segment

5. Determine the bending moment distribution factor (γ_r) for restraining segments A and B using Eq. 6 below.

$$\gamma_f = (1 - M_{mr}^2 / M_{crr}^2)_{A/B} \qquad (6)$$

where

M_{mr} = bending moment in restraining segment A or B from step 1
M_{cr} = elastic moment capacity in restraining segment A or B from step 2

6. Compute restraint stiffness for the critical segment, supporting segments, and split pipe stiffeners as shown in sub-steps a – d below.

    a. Critical segment weak axis flexural stiffness (α_{cy})

$$\alpha_{cy} = (n/2)EI_y / (k_y L_b) \qquad (7)$$

    where

    n = 4 if both ends are continuous or 3 if only one end is continuous

    b. Critical segment warping stiffness

$$\alpha_{cw} = EC_w / (k_y L_b) \qquad (8)$$

    Notice here that we use the effective length for weak axis restraint. This assumes the ratio of critical span to restraining span stiffness for both weak axis rotation and warping restraint are equal since we have a uniform cross section. Additionally this effective length is due to the warping stiffness of the restraining span and not any

warp restraining device, so if the restraining spans have a different cross section than the critical span, k_w for the restraining spans should be used.

c. Restraining segments A and B restraint stiffness

$$\alpha_{ryA/B} = \gamma_f EI_y/L_b(1 - \lambda_c/\lambda_r) \tag{9}$$

d. Split pipe warping restraint stiffness (if split pipe warp restraining device used)

$$\alpha_{pipe} = GJ_{pipe}d \tag{10}$$

where

d = distance between bottom and top flange centroids

7. Determine the stiffness ratios ($G_{A/B}$) for weak axis rotational restraint and warping at the A and B ends of the critical segment as shown in sub-steps a and b below.

a. Restraining segments A and B and pipe warping restraint stiffness ratio
$$G_{wA/B} = \alpha_{cw}/(\alpha_{pipe}) \tag{11}$$
Note that the warping stiffness of the restraining span should be added to the split pipe warping restraint if the restraining span warping stiffness is large enough to influence the ratio of stiffnesses in Eq. 11. In this study it was not.

b. Restraining segments A and B weak axis rotational restraint stiffness ratio

$$\alpha_{ryA/B} = \alpha_{cy}/\alpha_{ryA/B} \tag{12}$$

8. Solve for the effective length factors for weak axis rotation restraint (k_y) and warping (k_w) by using the appropriate restraint stiffness ratios and iterating to solve the equation below for k (Kavanagh, 1962). A G value of 50 may be used if one end of the critical span is free to warp or rotate about its weak axis (American Institute of Steel Construction, 2011).

$$\frac{G_A G_B}{4}\left(\frac{\pi}{k}\right)^2 + \left(\frac{G_A + G_B}{2}\right)\left(1 - \frac{\frac{\pi}{k}}{\tan\left(\frac{\pi}{k}\right)}\right) + \frac{2\tan\left(\frac{\pi}{2k}\right)}{\frac{\pi}{k}} = 1 \tag{13}$$

9. Determine the critical segment elastic bucking moment capacity (M_{cr}) using the effective length factors from step 13 and the bending coefficient, C_b, from step 2 in Eq. 2.

10. Iterate steps 1-9 until solution converges. Two iterations were sufficient for this study.

4. Parametric Study

A parametric study was used to verify the results of the proposed analytic solution using the three cross sections shown in Fig. 3 and the loading and span geometries shown in Fig. 4. Each combination of cross section as well as span and loading geometries were run in the three dimensional finite element program *ANSYS/Multiphisics® version 14.0* for critical span to depth ratios of 20, 25, 30, 35, and 40. At these ratios, the girder webs were not subject to significant distortion or buckling. The finite element model used in this study has been previously validated with full scale laboratory test results and additional analytic solutions (Quadrato, et al., 2010).

Every combination was run for girders with ½" thick plate bearing stiffeners and ½" thick pipe stiffeners with diameters 2" less than the girder flange width as shown in Fig. 5 (unless otherwise noted). ½" thick plate bearing stiffeners were also used under any concentrated loads. All specimens were loaded with unit loads and an eigenvalue buckling analysis was used to determine the critical buckling load. See Fig. 6 for an example buckled shapes. Critical spans in all cases were the spans with applied loads.
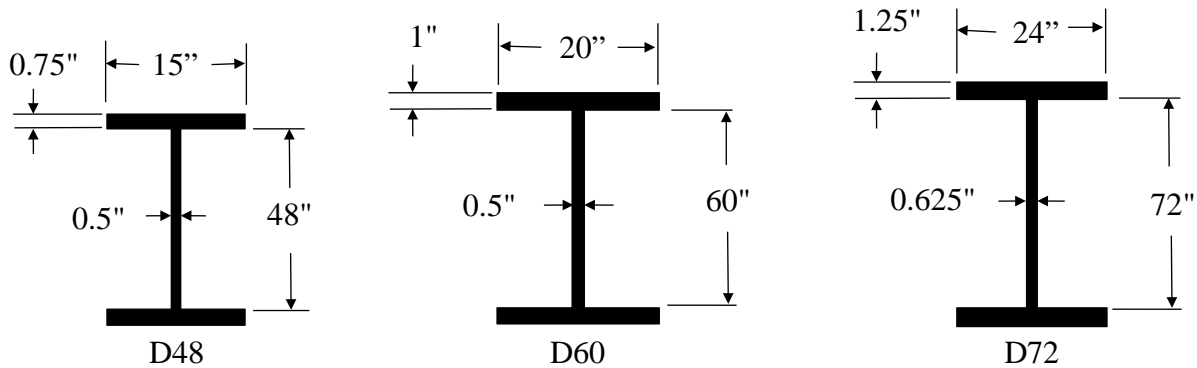
Figure 3: Cross Sections Used in Parametric Study
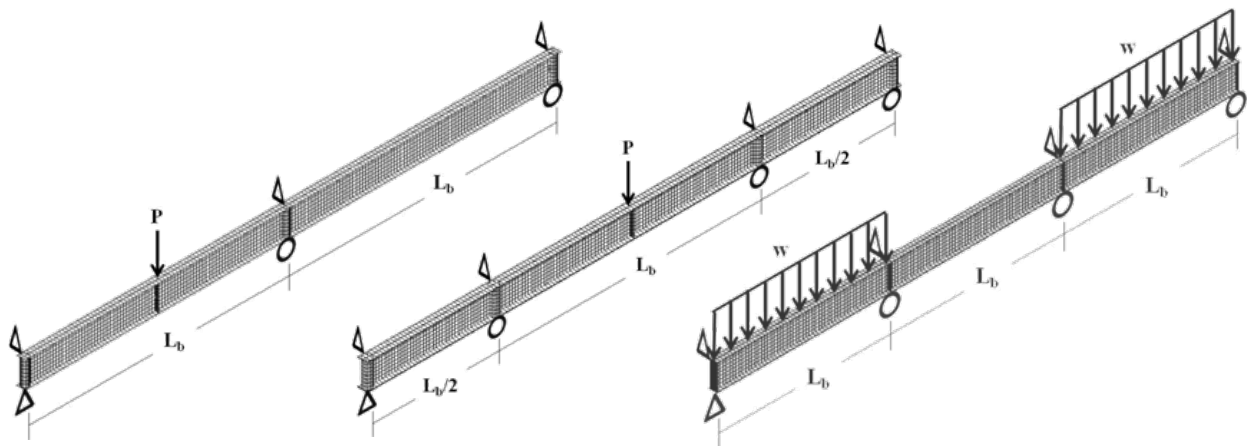
Figure 4: Span Geometries and Loading Used in Parametric Study
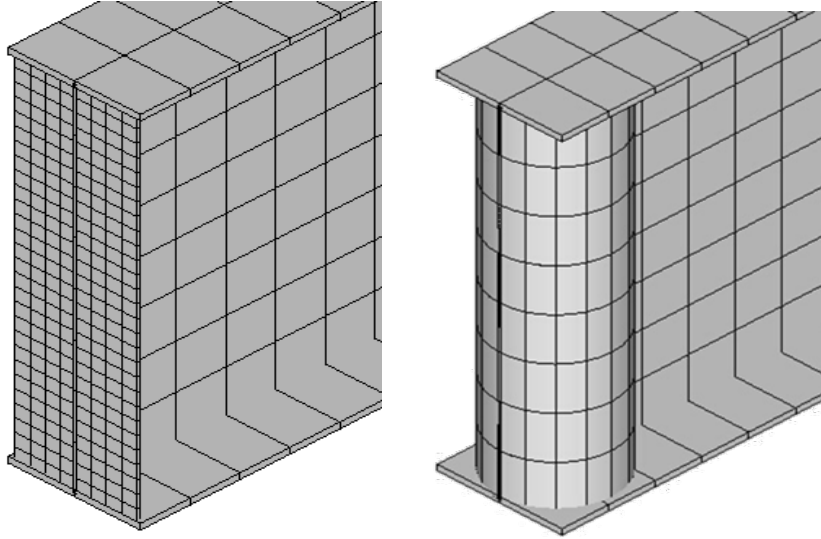
Figure 5: Plate Bearing Stiffener (L) and Pipe Bearing Stiffener (R) Details
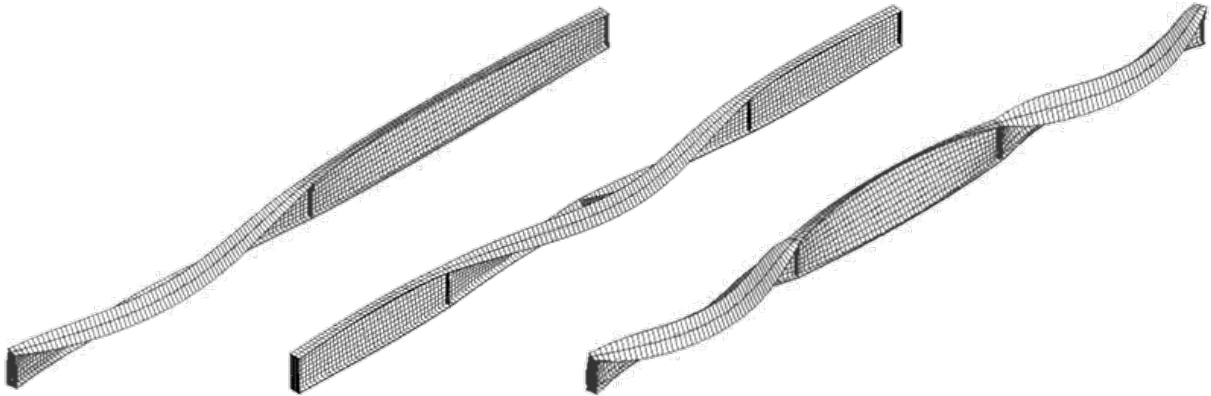
Figure 6: Sample Buckled Shapes for Plate Stiffener Specimens

5. Parametric Study Results

The figures below show the results for each of the load cases and span geometries considered. The critical buckling load results have been normalized by the simply supported span buckling load as calculated by Eq. 2 with k_y and $k_w = 1$. Note that the D72x24 specimen was run with a pipe diameter 4" less than its flange width, which is smaller than the pipe diameter relative to the flange width in the other two specimens. The purpose of this was to determine if the analytic procedure was able to adequately account for varying the pipe torsional stiffness.
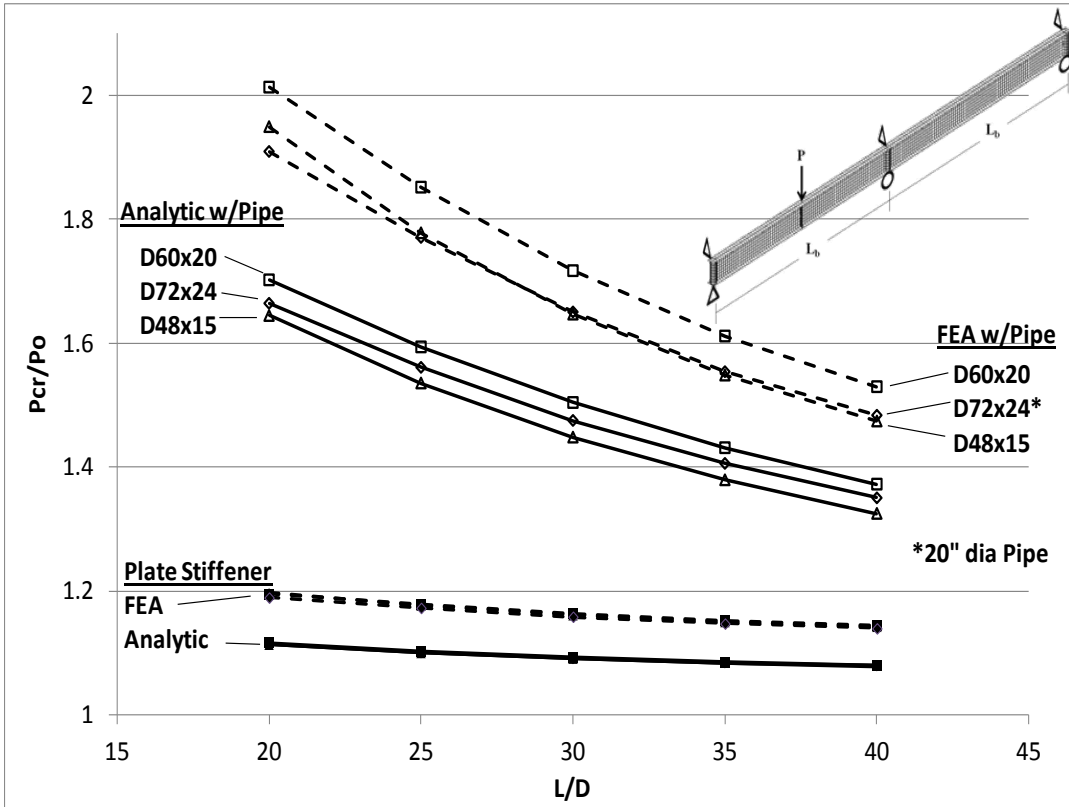
Figure 7: Buckling Loads for Two Span with Concentrated Load
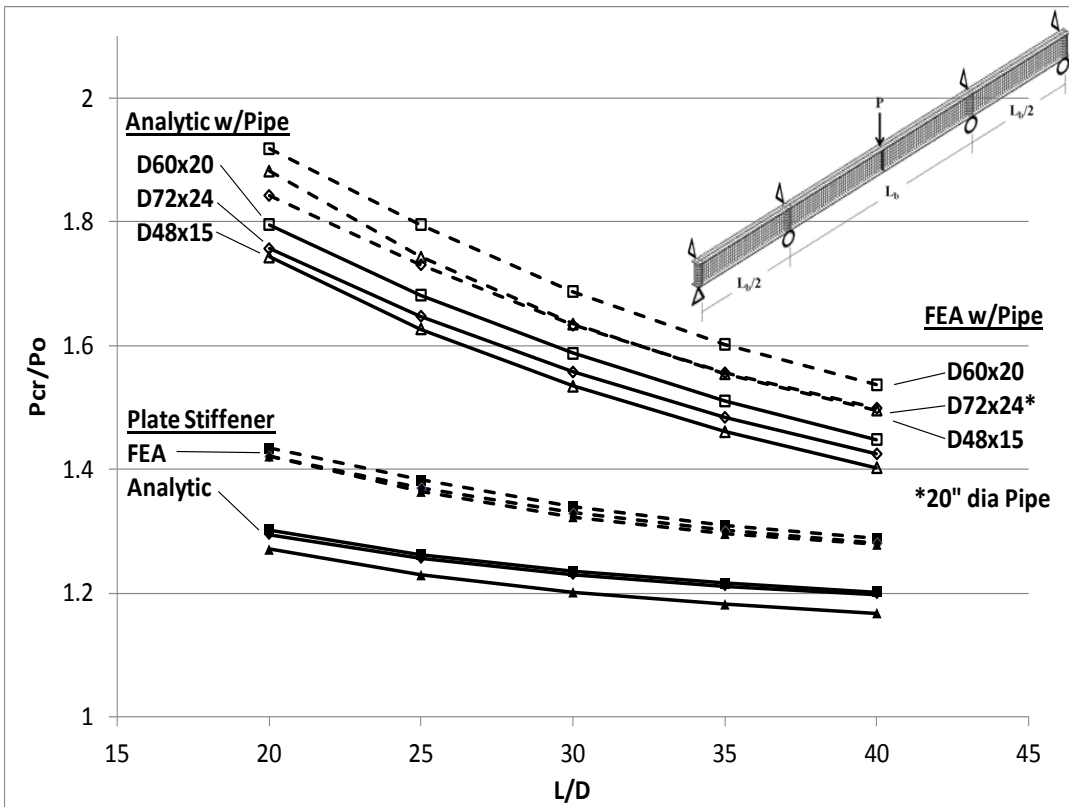
Figure 8: Buckling Loads for Three Span with Concentrated Load
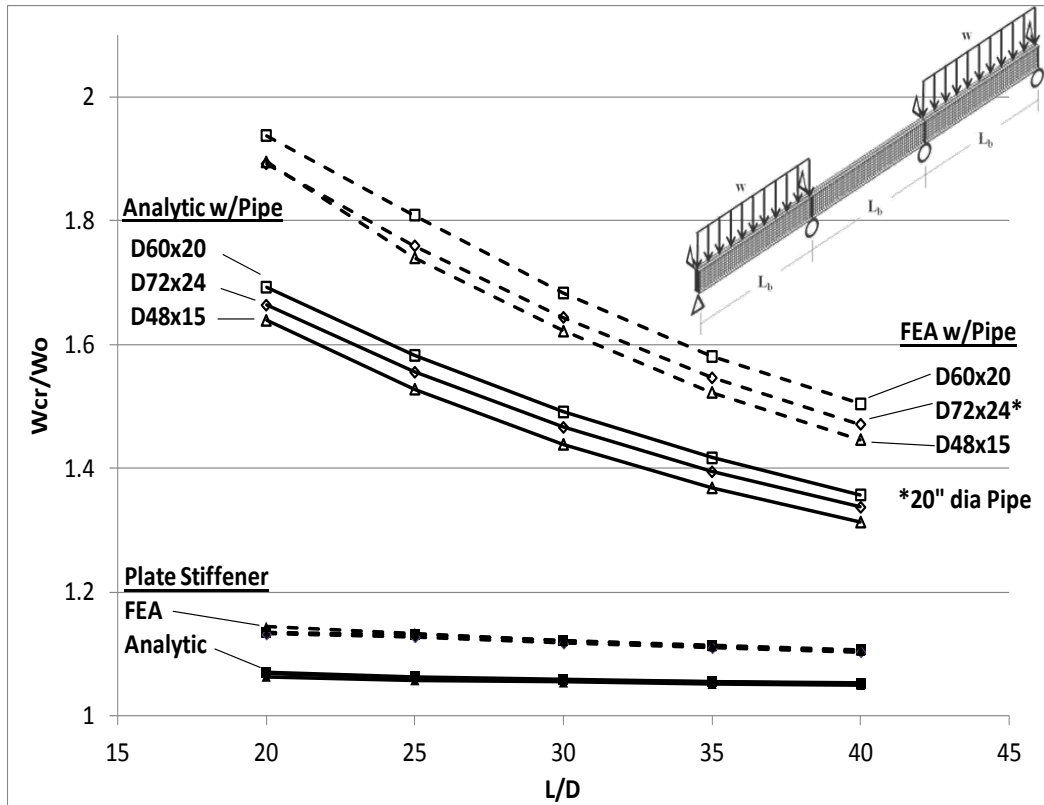
Figure 9: Buckling Loads for Three Span with Uniform Load

The results in Figs. 7 through 9 show that the proposed analytic solution provides a conservative yet reasonably accurate prediction of the increase in girder buckling strength and the corresponding critical unbraced length. Furthermore, as previously reported (Quadrato & Arnett, 2013), the split pipe stiffener significantly increases the critical buckling loads for continuous girders. Note that the interaction between spans is also relatively significant in increasing the critical span unbraced length.

The results also show that the proposed analytic solution error is relatively consistent for every case. For plate stiffened specimens the error is approximately 6% and is 15% for pipe stiffened specimens. This constant error is most likely due to inaccuracies in the moment magnification factor. Since the analytic model uses terms designed for a simply supported span, it should be expected that some error will be introduced that cannot be mitigated by iteration with respect to the relative stiffnesses to account for the girder continuity.

6. Conclusions

This study has proposed a reasonably conservative method to estimate continuous girder elastic buckling using split pipe or plate bearing stiffeners. The study investigated all combinations of three doubly symmetric girder cross sections, three span and load geometries, and five span-to-depth ratios for girders using plate and split pipe bearing stiffeners. Errors in the proposed analytic solution, when compared to a previously validated finite element model, were approximately 5% in the plate bearing stiffener specimens and 15% in pipe bearing stiffener

specimens. All errors were conservative and consistent. The results also showed an approximate 15% to 20% increase in elastic buckling capacity for the plate stiffened girders and 30% to 100% for the pipe stiffened specimens.

Future work will focus on varying loading conditions including those found in typical bridge construction, such as distributed loading over positive moment regions as is common during deck placement, to determine if the proposed analytic procedure can be adjusted to accommodate these applied loads. Additionally, the impact of intermediate bracing patterns between the abutments and piers will be investigated to determine how the associated critical unbraced lengths are impacted by the presence of pipe stiffeners in continuous girders.

Acknowledgements

References

American Institute of Steel Construction. (2011). *Manual of Steel Construction.* Chicago: American Institute of Steel Constrution.

Kavanagh, T. (1962). Effective Length of Framed Columns. *Transactions of the American Society of Civil Engineers , 127*, 81-101.

Nethercot, D., & Rockey, K. (1971). A Unified Approach to the Elastic Lateral Buckling of Beams. *The Structrual Engineer , 49* (7), 321-330.

Pi, Y.-L., & Trahair, N. S. (2000). Distortion and Warping at Beam Supports. *Journal of Structural Engineering ,* 1279-1287.

Quadrato, C. E., & Arnett, K. P. (2013). Calculating the Impact of Partial Warp Restraint on Steel Girder Elastic Buckling Strength. *Proceedings of the Annual Stability Conference.* Grapevine: Structural Stability Research Council.

Quadrato, C., Wang, W., Battistini, A., Wahr, A., Helwig, T., Frank, K., et al. (2010). *Technical Report 0-5701-1 Cross-Frame Connection Details for Skewed Steel Bridges.* Austin: Center For Transportation Research.

Structural Stability Research Council. (1998). *Guide to Stability Design Criteria for Metal Structures.* (T. Galambos, Ed.) New York: John Wiley & Sons.

Trahair, N. S. (1993). *Flexural-Torsional Buckling of Structures.* Boca Raton: CRC Press.